

A Machine Learning Based Classification Approach for Power Quality Disturbances Exploiting Higher Order Statistics in the EMD Domain

Faeza Hafiz^{*} and Celia Shahnaz[†]

Department of Electrical and Electronic Engineering,
Bangladesh University of Engineering and Technology, Dhaka, Bangladesh
E-mail: ^{*} faezahafiz@gmail.com, [†] celia@eee.buet.ac.bd

Abstract: The aim of this paper is to propose a new approach for the pattern recognition of power quality (PQ) disturbances based on Empirical mode decomposition (EMD) and k Nearest Neighbor (k -NN) classifier. Since EMD decomposes a signal into intrinsic mode functions (IMF) in time-domain with same length of the original signal, it preserves the information that is hidden in Fourier domain or in wavelet coefficients. In this proposed method, power signals are decomposed into IMFs in EMD domain. Due to the presence of non-linearity and noise on the original signal, it is hard to analyze them by second order statistics. Thus, an effective feature set is developed considering higher order statistics (HOS) like variance, skewness, and kurtosis from the decomposed first three IMFs. This feature vector is fed into different classifiers like k -NN, probabilistic neural network (PNN), and radial basis function (RBF). Among all the classifiers, k -NN showed higher classification accuracy and robustness both in training and testing to detect the PQ disturbance events. Simulation results evaluated that the proposed HOS-EMD based method along with k -NN classifier outperformed in terms of classification accuracy and computational efficiency in comparison to the other state-of-art methods both in clean and noisy environment.

1 Introduction

Reliable power supply is one of the a major concern for smart grids due to the rapid inclusion of sensitive loads into the power system. Degradation of reliability in power system arises because of various reasons, like power-line disturbances, malfunctions, instabilities, short lifetime, failure of electrical equipment, intermittency of distributed energy resources, and so on. All of these reasons can be detected analyzing the voltage/current signals of the power system. For example, faults in a distribution system shows sag or momentary interruption in voltage signals, sudden drop off large load or energization of a large capacitor bank cause swell in voltage, harmonic distortion occurs due to the inclusion of power electronic inverters or solid-state switching devices, capacitor or transformer switching leads to transients, sudden higher load inclusion impacts are seen as flickers, lightning strikes causes spikes in the voltage signal [1], [2].

In order to ensure an improved power delivery to the customers, utility companies need to know the reasons of disturbances to resolve the issues. Thus it is important for the utility companies to detect the problem from the signals at hand so that they can take mitigation actions within short period of time. In this regard, researchers are interested recently to use efficient and appropriate signal processing methods to extract all the the important information to classify the PQ disturbance events. Most of the proposed research works are based on extracting all the information from a signal into a set of features. Then they utilized different classification methods to obtain the accurate class of a signal based on the feature set. As a result, the identification process of PQ disturbance events follows three steps, signal analysis or decomposition, feature vector selection; and train a classifier to accurately classify the disturbance [3].

According to the above statement, the available power disturbance time series data is processed through different signal processing approaches in the first step of PQ disturbance classification. Considering this objective, several signal processing transformation methods were proposed in the literature. Among all of them, fourier transform (FT) was most commonly used [4], which is only applicable to the stationary signals. To obtain time frequency information

from the PQ disturbance waveform, short time fourier transform (STFT) was proposed in [5–7]. The limitation of STFT is that it can not extract transient signal information properly due to fixed window size selection. Different wavelet based transformations, like wavelet transformation, wavelet packet transformation, and wavelet multiresolution analysis were analyzed in [8–14]. These proposed wavelet domain based methods are dependent on proper selection of mother wavelet and the level of decomposition for effective recognition of disturbance signals. Stockwel transform was proposed in [15, 16]. It uniquely combines a frequency dependent resolution and simultaneously localizes the real and imaginary spectra. But similar to the STFT, it requires the selection of a suitable window size to match with the specific frequency content of the signal. In [17], the authors described a Hilbert transform based signal decomposition for the feature extraction from the distorted waveform to generate an analytical signal. But Hilbert Transformer provided a better approximate of a quadrature signal only if the signal reached into a narrow band condition. A combination of Prony analysis and Hilbert transform was also considered in [18], where a signal was reconstructed using linear combination of damped complex exponential. A prediction model was also developed in this work to estimates the different modes of a signal. The estimated signal best fits with the original signal only if condition of minimization of least square error between the original signal and estimated signal was satisfied. One limitation of this method is that the number of mode is required to be selected beforehand for the Prony analysis and no rules were developed to guide the selection procedure of this numbers. Considering these limitations of other methods, we prefer to utilize empirical mode decomposition (EMD) method in this work for PQ disturbance signal analysis. Since EMD is a multi-resolution signal decomposition technique, it has the ability to denoise signals and detect PQ disturbances accurately [19, 20]. In EMD, the intrinsic oscillatory modes of a signal is identified primarily in time scale. Then the signal is decomposed into intrinsic mode functions (IMFs) according to the oscillatory modes. EMD is adaptive with the basic functions which are derived from the data. The computation of EMD does not require

Table 1 Models of power quality disturbance signals

Disturbance	Equations	Parameters
Normal	$v(t) = V \sin \omega_c t$	$u(t)$ is the unit function
Sag	$v(t) = V[1 - \gamma\{u(t - t_1) - u(t - t_2)\}] \sin \omega_c t$	$0.1 \leq \gamma \leq 0.9$, $T \leq (t_2 - t_1) \leq 9T$
Swell	$v(t) = V[1 + \gamma\{u(t - t_1) - u(t - t_2)\}] \sin \omega_c t$	$0.1 \leq \gamma \leq 0.9$, $T \leq (t_2 - t_1) \leq 9T$
Flicker	$v(t) = V[1 + \gamma \sin(2\pi\beta t)] \sin \omega_c t$	$0.1 \leq \gamma \leq 0.2$, $5 \text{ Hz} \leq \beta \leq 20 \text{ Hz}$
Interruption	$v(t) = V[1 - \gamma\{u(t - t_1) - u(t - t_2)\}] \sin \omega_c t$	$0.9 \leq \gamma \leq 1$, $T \leq (t_2 - t_1) \leq 9T$
Transient	$v(t) = V[\sin \omega_c t + \gamma e^{-(t - t_1)/\tau} \sin\{2\pi f_n(t - t_1)\}\{u(t_2) - u(t_1)\}]$	$0.1 \leq \gamma \leq 0.9$, $0.5T \leq (t_2 - t_1) \leq 3T$, $300 \text{ Hz} \leq f_n \leq 900 \text{ Hz}$, $8 \text{ ms} \leq \tau \leq 40 \text{ ms}$
Harmonics	$v(t) = V[\sin \omega_c t + \gamma_3 \sin 3\omega_c t + \gamma_5 \sin 5\omega_c t]$	$0.1 \leq \gamma \leq 0.9$, $T \leq (t_2 - t_1) \leq 9T$, $0.05 \leq \gamma_3, \gamma_5 \leq 0.15$
Sag with Harmonics	$v(t) = V[1 - \gamma\{u(t - t_1) - u(t - t_2)\}] * [\sin \omega_c t + \gamma_3 \sin 3\omega_c t + \gamma_5 \sin 5\omega_c t]$	$0.1 \leq \gamma \leq 0.9$, $T \leq (t_2 - t_1) \leq 9T$, $0.05 \leq \gamma_3, \gamma_5 \leq 0.15$
Swell with Harmonics	$v(t) = V[1 + \gamma\{u(t - t_1) - u(t - t_2)\}] * [\sin \omega_c t + \gamma_3 \sin 3\omega_c t + \gamma_5 \sin 5\omega_c t]$	$0.1 \leq \gamma \leq 0.9$, $T \leq (t_2 - t_1) \leq 9T$, $0.05 \leq \gamma_3, \gamma_5 \leq 0.15$
Spike	$v(t) = V[\sin \omega_c t - \text{sign}(\sin \omega_c t) \times \{\sum_{n=0}^9 \kappa \times \{u(t - (t_1 + 0.02n)) - u(t - (t_2 + 0.02n))\}\}]$	$0.1 \leq \kappa \leq 0.4$, $0 \leq (t_2, t_1) \leq 0.5T$, $0.01T \leq (t_2 - t_1) \leq 0.05T$
Notch	$v(t) = V[\sin \omega_c t + \text{sign}(\sin \omega_c t) \times \{\sum_{n=0}^9 \kappa \times \{u(t - (t_1 + 0.02n)) - u(t - (t_2 + 0.02n))\}\}]$	$0.1 \leq \kappa \leq 0.4$, $0 \leq (t_2, t_1) \leq 0.5T$, $0.01T \leq (t_2 - t_1) \leq 0.05T$

any previously known value of the signal. As a result, EMD is especially applicable for nonlinear and non-stationary signals, such as PQ disturbances.

Features selection is the key element among the three steps for PQ disturbance classification. Inappropriate feature selection adds difficulty to the classification. Previous studies overlooked some essential features [21–24]. In this work, we endeavor to develop appropriate features selection to improve the efficiency of classification. Higher order statistics (HOS) of the extracted IMFs, such as variance, skewness and kurtosis are considered in this regard to form the feature vector. First and second order statistics can not extract the phase information of a signal and can easily be affected by noises, HOS are less effected by background noise and contain phase information. The discriminatory attributes of the HOS for different PQ disturbance signals are more prominent in the EMD domain as seen from the shape of the histograms of the IMFs and the values of the corresponding HOS [25, 26]. Thus, it is expected that HOS of PQ disturbances would be more effective if they are computed in the EMD domain rather than in the time domain.

Recently reported works applied different machine learning algorithms to classify PQ disturbances after defining the feature vectors from the disturbance waveform. Probabilistic neural network [9], radial basis function neural network [23], k -nearest neighbour [27], support vector machines [28] and decision tree[29] were mostly utilized classifiers for PQ disturbance signals. In this research, IMFs of the PQ disturbance signals are obtained by using EMD operation. As most frequency content of the PQ disturbance signals lies in the first three IMFs, they are selected for further analysis [30]. HOS of the extracted IMFs, such as variance, skewness and kurtosis are extracted to form the feature vector. The feature set obtained is fed to the radial basis function (RBF), probabilistic neural network (PNN) and k nearest neighbor (k -NN) classifiers for classifying the multi

class PQ disturbance signals. For the characterization of PQ disturbance signals, mathematical models of eleven classes of disturbances are used. In comparison to the other methods, k -NN classifiers shows superior performance for the proposed HOS of EMD (HOS-EMD) based feature vector. Simulation results reveal the effectiveness of the HOS-EMD method for classifying multi-class PQ disturbance signals.

This paper is organized as follows. The proposed higher order statistics based feature extraction of PQ disturbance signal in EMD domain termed as HOS-EMD method is discussed in Section II. This section includes a brief background of PQ disturbances signal models, how IMFs are generated in EMD domain, feature selection from IMFs, and brief description of k -NN, PNN, and RBF classifiers. The simulation results of the HOS-EMD classification method are provided and its performance are compared relative to the other methods in section III. The importance of the proposed method are highlighted in section IV with concluding remarks.

2 HOS-EMD METHOD

In power system, a pure voltage or current is a sinusoidal signal that can be mathematically represented as

$$v(t) = V \sin \omega_c t \quad (1)$$

where, V and f represent the amplitude and fundamental frequency respectively. Different types of power quality disturbance signal like sag, swell, fluctuation, interruption, transient, harmonics, sag with harmonics, swell with harmonics, spike and notch can be seen in power system. The mathematical models of these disturbance signals are provided in Table 1. To classify these signals, proposed

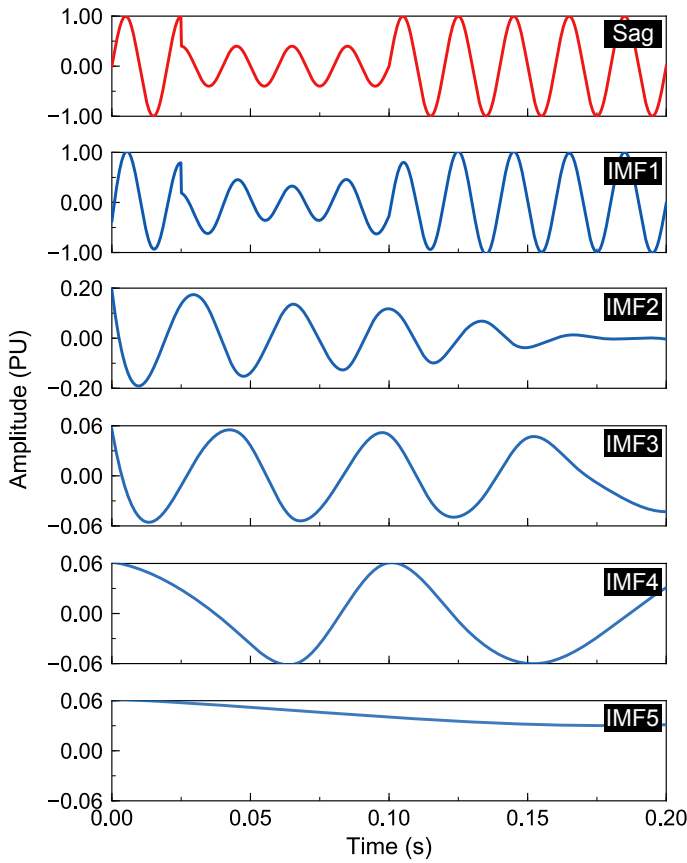


Fig. 1: Voltage sag and its intrinsic mode functions.

HOS-EMD method follows two steps, namely feature extraction and classification. The details of these steps are described below.

2.1 Feature Extraction

2.1.1 Empirical Mode Decomposition: EMD is a method that decomposes a signal into multiple IMFs in time domain. As it preserves the domain during decomposition, there is less probability to lose important information from a signal. To decompose a signal into IMFs, the following mandatory conditions are needed to be satisfied.

Condition 1: The total number of local minima and maxima should be equal or differ at most one compared to the number of zero crossings in the whole dataset of the signal.

Condition 2: Mean values of the local minima and local maxima envelope must be zero.

A brief description of the IMF decomposition is illustrated below.

1. All the local maxima and minima are determined from the given signal data.
2. These data are connected to construct upper and lower envelope of the signal using by cubic spline lines.
3. The mean of the envelopes are calculated as m_1 .
4. The difference between the PQ disturbance signal, $v(t)$ and m_1 are calculated as-

$$e_1(t) = v(t) - m_1 \quad (2)$$

If this difference, $e_1(t)$ satisfies the conditions of IMF described above, then it can be considered as first frequency and amplitude modulated oscillatory mode of $v(t)$.

5. If $e_1(t)$ is not an IMF, then it is passed through the second sifting process, where steps i-iv are repeated on $e_1(t)$ to obtain another component $e_2(t)$ by following the equation below:

$$e_2(t) = e_1(t) - m_2 \quad (3)$$

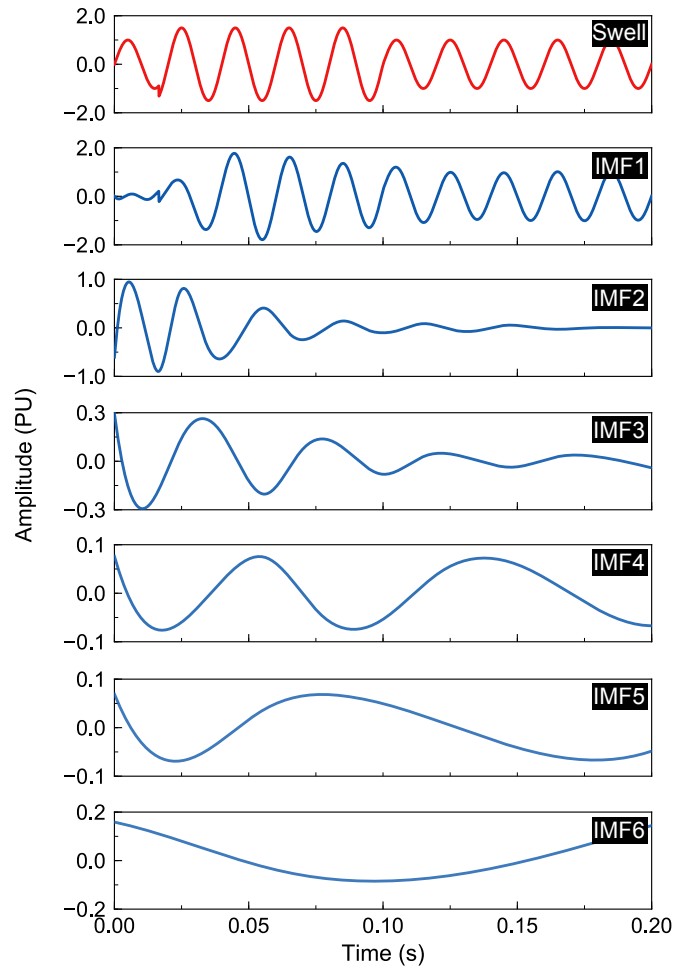


Fig. 2: Voltage swell and its intrinsic mode functions.

where m_2 is the mean of upper and lower envelopes of $e_1(t)$.

6. Let after w cycles of operation, $e_w(t)$, is calculated as

$$e_w(t) = e_{w-1}(t) - m_w \quad (4)$$

and it satisfies the IMF conditions. The the first IMF component of the original signal will be $I_1(t) = e_w(t)$.

7. $I_1(t)$ is then subtracted from $v(t)$, and the residual signal, $r_1(t)$ is calculated as

$$r_1(t) = v(t) - I_1(t) \quad (5)$$

This residual signal, $r_1(t)$ is then treated as the original data for calculating the next IMF.

8. The stopping criteria of the sifting process is calculating the standard different of two consecutive signal and check with some threshold level. Let after repeating steps i-vii for W times, W no. of IMFs is obtained along with the final residue $r_w(t)$ are obtained. Then the standard difference (SD) is calculated as:

$$SD = \sum_{w=2}^W \frac{|e_{w-1}(t) - e_w(t)|^2}{e_w(t)^2} \quad (6)$$

where, the index terms, w and $w - 1$ are indicating two consecutive sifting processes. Thus the decomposition process is stopped since $r_w(t)$ becomes a monotonic function from which no more IMF can be extracted. To this end, for W level of decomposition, the PQ disturbance signal $v(t)$ can be reconstructed by the following formula,

$$v(t) = \sum_{w=1}^W I_w(t) + r_w(t) \quad (7)$$

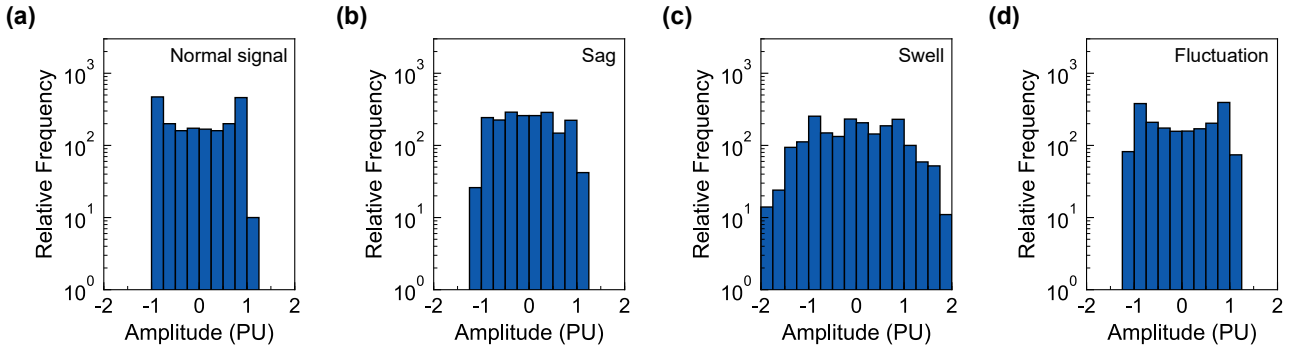


Fig. 3: Histogram of first IMF of power quality disturbances. (a) normal signal, (b) sag, (c) swell, and (d) fluctuation

2.1.2 IMF Selection: While decomposing all the PQ disturbance signals through EMD process, sag and swell always results in six IMFs and harmonics and fluctuation signals are decomposed into one or two IMFs. The IMFs for sag and swell are shown in Fig. 1 and Fig. 2. It is found that frequency contents of a signal are mostly available in the first three IMFs. IMFs become smoother with the increase of their level according to these figures. Thus, we can extract necessary information from first few IMFs instead of considering all of the available IMFs. Eventually, it will help to reduce the requirement of memory and speed up the calculation process for classifiers. Considering this observation, we are motivated to exploit the first three IMFs for feature selection in this work. IMFs are considered as zero for the signals which are decomposed into less than three IMFs.

2.1.3 Higher Order Statistics: Distribution of a data set can be understandable easily by analyzing its level of dispersion, asymmetry and concentration around the mean. Calculation of HOS is an effective way to measure these information, especially for the systems with nonlinear dynamics. They perform better to extract information than the second order statistics with the presence of noise in the signal. In this work, HOS are termed as variance, skewness and kurtosis. From the first three IMFs after decomposition of a PQ disturbance signal in EMD domain, their variance, skewness and kurtosis are calculated as a feature vector for classifying the PQ disturbance signals. For an N -point data, v_1, v_2, \dots, v_N , the corresponding variance (σ^2), skewness (α_1) and kurtosis (α_2) are calculated as

$$\sigma^2 = \frac{1}{N} \sum_{n=1}^N (v_i - \mu)^2; \mu = \frac{1}{N} \sum_{n=1}^N (v_i) \quad (8)$$

$$\alpha_1 = \frac{1}{N} \sum_{n=1}^N \left(\frac{v_i - \mu}{\sigma} \right)^3 \quad (9)$$

$$\alpha_2 = \frac{1}{N} \sum_{n=1}^N \left(\frac{v_i - \mu}{\sigma} \right)^4 \quad (10)$$

here, μ symbolizes the sample mean of the data. For a symmetric distribution of data about mean, the skewness is zero. Positive skewness occurs when data are spread towards the right of the mean. When data is spread more to the left of the mean, then skewness becomes negative. Kurtosis provides the idea of whether a dataset are heavy-tailed or light-tailed compared to a normal distribution. If distribution of signal is light-tailed, then the kurtosis is less than zero and it becomes greater than zero when the distribution has heavier tails. Figure 3 shows the histograms of the first IMF of pure signal and three PQ disturbances. From the figures, it is observable that the shapes of the PQ disturbances are different from each other. It is expected that the values of the corresponding variance, skewness and kurtosis are different from each other as these values are delivering the information of the dispersion, asymmetry and tailedness of data. Due to decomposition of the signal into IMFs, HOS based features

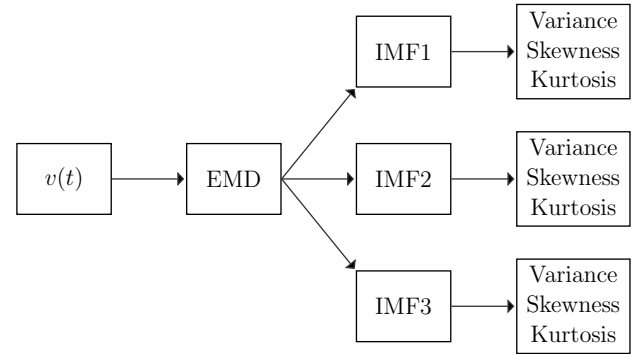


Fig. 4: Feature Extraction from distorted waveform

becomes more prominent in the EMD domain rather than in spatial domain for classifying the PQ disturbance signals. Thus, from the first three extracted IMFs, nine features are derived for the feature vector. Figure 4 shows the flow diagram for proposed extracted features from the distorted waveform.

2.2 Classification

2.2.1 k-NN Classification: k -NN is a simple and robust classifier [27]. In this algorithm, k neighborhood is defined by the user. For a testing sample, a class is assigned by checking more frequent training samples in the k neighborhood. The value of k is required to be varied to find the match class between training and testing data. The default value of k is 1. In this paper, we varied the value of k from 1 to 10 and the best match is considered. We used euclidean distance to find the object similarity in the k neighborhood as shown in (10).

$$d(y_n) = \frac{1}{1 + e^{-y_n}} \quad (11)$$

2.2.2 Probabilistic Neural Network: Similar to the k NN classifier, probabilistic neural networks (PNNs) classifier is a supervised learning classifier. But it follows distinct algorithm which is discussed below [9].

- PNN utilizes the probabilistic model with a Gaussian mapping function.
- It does not need to set initial weights of the network. But the spread of the Gaussian function is required to be specified.
- There is no relationship between the learning and recalling processes.
- Weights of the network do not change with the difference between the inference vector and the target vector.

Figure 5 shows architecture of PNN model composed of input, hidden and output layers. For a classification problem, the training

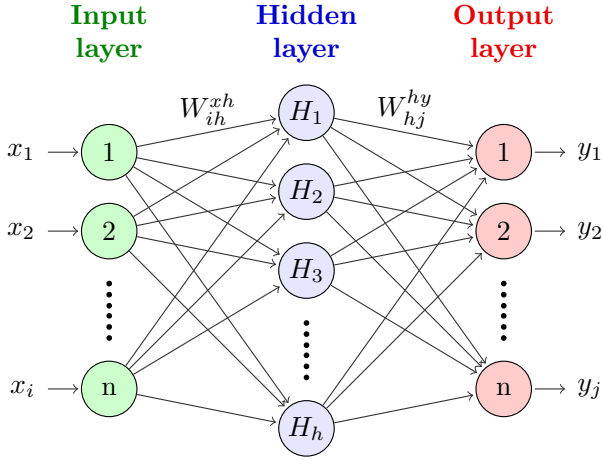


Fig. 5: Architecture of PNN neural network

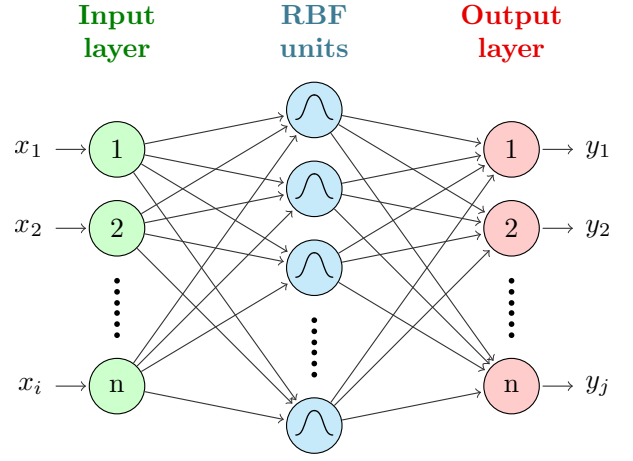


Fig. 6: Architecture of RBF neural network

data is classified according to their distribution values of probabilistic density function (PDF). A PDF is shown as follows

$$f_r(x) = \frac{1}{N_r} \sum_{j=1}^{N_r} \exp \left(\frac{-(\|X - X_{rj}\|)^2}{2\sigma^2} \right) \quad (12)$$

Modifying and applying eq. (12) to the output vector H of the hidden layer in the PNN is as

$$H_h = \exp \left(\frac{-\sum_i (X_j - W_{ih}^{xh})^2}{2\sigma^2} \right) \quad (13)$$

$$net_j = \frac{1}{N_r} \sum_h W_{hj}^{hy} H_h \text{ and } net_j = \max_r(net_r) \quad (14)$$

then $y_j = 1$ or $y_r = 0$, where

i = number of input layers;

h_j = number of hidden layers;

j = number of output layers;

r = number of training examples;

N = number of classifications (clusters);

σ = smoothing parameter (standard deviation);

X = input vector;

$\|X - X_{rj}\|$ = Euclidean distance between the vectors X and X_{rj} ;
i. e. $\|X - X_{rj}\| = \sqrt{\sum_i (X - X_{rj})^2}$

W_{ih}^{xh} = connection weight between the input layer X and the hidden layer H

W_{hj}^{hy} = connection weight between the hidden layer H and the output layer Y

2.2.3 Radial Basis Neural Network : RBF network consists of an input layer, a hidden layer that uses radial basis functions as activation function, and linear combination of set of weights W in the output layer. The schematic diagram of RBF neural network is shown in Fig. 6. The transfer functions in the nodes are similar to the multivariate Gaussian density function:

$$\Phi_j(x) = \exp \left(\frac{\|x - \mu_j\|^2}{2\sigma_j^2} \right) \quad (15)$$

here x is considered as input vector, μ_j and σ_j are the center and spread of the multivariate Gaussian function. Each RBF unit has a significant activation function that defines a specific region. This region is determined by μ_j and σ_j . As a result, RBF defines unique local neighborhood in the input space. The connections between the activation layer and the output layer is the linear weighted summation of the RBF units. Thus, the value of k^{th} output node, y_k is followed by given equation:

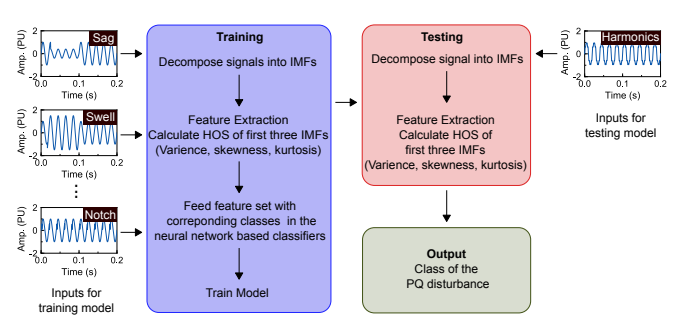


Fig. 7: Overall Method

$$y_k(x) = \sum_{j=1}^h \zeta_{kj} \Phi_j(x) + \zeta_{k0} \quad (16)$$

here ζ_{kj} is the connection weight between the k^{th} output and the j^{th} activation layer. ζ_{k0} is the basis term.

To get the overview of the proposed method, steps discussed above are depicted in Fig. 7.

3 SIMULATION RESULT AND ANALYSIS

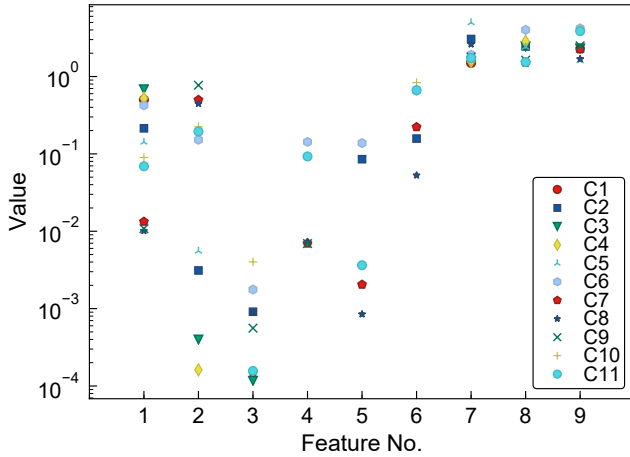
For simulation, eleven classes of PQ disturbance signals were generated using in MATLAB considering the equations in Table I with a sampling frequency of 2 kHz. For convenience, the PQ disturbance signals were termed as:

1. C1- Normal,
2. C2- Sag,
3. C3 - Swell,
4. C4 - Fluctuation,
5. C5 - Interruption,
6. C6 - Transient,
7. C7 - Harmonics,
8. C7 - Sag with harmonics,
9. C8 - Swell with harmonics,
10. C10 - Spike,
11. C11 - Notch.

The effectiveness of the proposed method are described in following subsections.

Table 2 Values of Pure Signals

Classes	Variance	Skewness	Kurtosis
C1	0.5	2.77E-16	0.375
C2	0.167	1.11E-18	0.304
C3	0.6594	8.19E-18	0.6358
C4	0.5147	9.36E-04	0.7302
C5	0.45	1.78E-17	0.27
C6	0.5287	0.152	0.3586
C7	0.5	2.66E-16	0.4453
C8	0.3734	7.78E-18	0.189
C9	0.6186	1.61E-16	0.6304
C10	0.5114	0.0027	0.3997
C11	0.4781	0.0059	0.3391

**Fig. 8:** Separability of the HOS-EMD based features in logarithmic scale.

3.1 Statistical Analysis of the Feature Extraction

For the purpose of signal analysis, each PQ disturbance signals are decomposed into IMFs using the algorithm described in subsection 2.1. Then HOS are calculated from the first three IMFs. The impact of decomposition in the EMD domain becomes visible while comparing with the HOS values of the original PQ disturbance signals. Table 2 and Fig. 8 show the HOS values obtained for different PQ disturbance signals and their first three IMFs, respectively. In Fig. 8, the stamps of the feature set considered in x-axis are variance, skewness, and kurtosis of first three IMFs of different PQ disturbance signals, respectively. For clarification, feature stamp 1, 2 and 3 are the variance, skewness and kurtosis of first IMF. Similarly, variance, skewness, and kurtosis of second IMF are considered as stamp no. 4, 5, and 6; and third IMF are 7, 8, and 9. Corresponding feature values are shown in logarithmic scale in y-axis. From Table 2, it can be seen that variance, skewness and kurtosis of the original signals for different PQ disturbances are very close to each other. On the other hand, it is clear that the HOS values are distinguishable in EMD domain for different classes of PQ signals from Fig. 8. Since the separability of the PQ disturbances are larger for IMFs than the original signals, the proposed feature set is more robust to differentiate them. It is also clear that with the increase of IMF level, the separability of the features reduces.

3.2 Comparative Analysis with Other Methods

Machine learning based classifiers are required to be trained with large amount of data before testing. Due to unavailability of required amount of database for different classes of PQ disturbance, the classifiers are trained with synthetic data which are generated using the mathematical models along with the random variation of parameters like amplitude (γ), frequency(β), duration(t_1, t_2) which are

described in Table 1. To evaluate the performance of the proposed HOS-EMD method for classification of eleven PQ events, a total of 1485 signals with 135 signals of each class are generated. The fundamental frequency of the signals is 50 Hz. Among 135 signals for each class, 35 signals are utilized for training and the rest of the signals are considered for testing and validation. The performance evaluation are done based on confusion matrix and overall efficiency in percentage (%) calculation. Confusion matrix is a form of representing the result from a classification exercise. Overall efficiency is calculated using the formula given as follows-

$$\text{Overall Efficiency} = \frac{\text{No. of correctly classified events}}{\text{Total no. of events}} \quad (17)$$

For same type of training and testing data a comparative study between S -transform [31], Hilbert-Huang transform (HHT) [32], and proposed HOS-EMD is made. Confusion matrix resulting from the proposed feature set and compared methods set via k -NN classifier are presented in Fig. 9.

It can be seen from the diagonal entries of confusion matrix in Fig. 9 (a) that S -transform is unable to distinguish among PQ disturbance signals, such as swell (C3), fluctuation (C4), harmonics (C7), swell with harmonics (C9), spike (C10) and notch (C11). Overall accuracy for S -transform is 81.2% which is shown in Fig. 10 (a). It is also notable from Fig. 9 (b) that HHT based k -NN classification misclassifies some sag (C2), interruption (C5), harmonics (C7) and sag with harmonics (C8) signals. Compared to the S -transform, HHT improves the classification accuracy up to 96%. The accuracy level for HHT is depicted in Fig. 10 (b). Fig. 9 (c) shows that HOS-EMD method based features are able to identify all of the signals almost perfectly. Overall accuracy level is reached up to 99%. According to Fig. 10 (c), error level is reduced for the proposed HOS-EMD method compared to the S -transform and HHT method.

3.3 Classifiers Efficiency Analysis

Classification performance in terms of overall efficiency (%) when fed to RBF, PNN and k -NN classifiers are calculated for all classes. They are presented in Fig. 11 (a). It is visible that for the selected three classification methods, S -transform performs poorly compared to HHT and proposed HOS-EMD method. For RBF classifiers, HHT performed better compared to S -transform and HOS-EMD method. But for PNN and k -NN classifiers, HOS-EMD method outperformed compared to HHT and S -transform. Overall classification accuracy increases for PNN and k -NN classifiers compared to RBF during the application of HHT and HOS-EMD. Simulation analysis was also performed by increasing the training and testing data (70 data for training and 200 data for testing). Due to the increase of training data, classification accuracy increased for all of the methods and classifiers according to Fig. 11 (b). Similar to the previous scenario, S -transform performs poorly compared to the other methods. Though HHT performed better while utilizing RBF, overall classification accuracy increased up to 99.6% while HOS-EMD and k -NN classifier is used.

It should be noted that the structure of k -NN is simple and it requires less learning time requirement compared to PNN and RBF. The time requirement for training and testing are also specified in Fig. 11 (c). It is clarified that with the nine features resulting from HOS-EMD domain with k -NN classifier requires less time for computation compared to RBF and PNN classifiers. Overall, k -NN classifier effectively classifies different kinds of PQ disturbances.

3.4 Performance of k -NN under Noisy Environment

In an electrical power distribution network, the practical data consists of noise. Therefore, the proposed approach has to be analyzed under noisy environment. Gaussian noise is widely considered in the research for power quality issues [19, 20]. Thus simulation is also performed with the addition of noise with pure signals and analyzed with EMD-transform for the HOS based feature extraction. k -NN is trained and subsequently tested for classification after the extraction

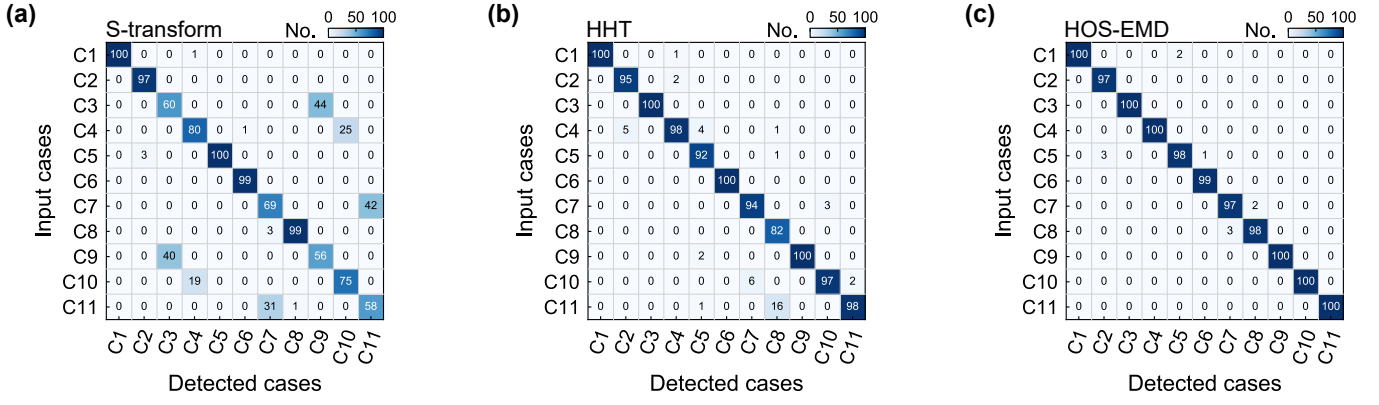


Fig. 9: Confusion matrix of different methods: (a) S-transform, (b) HHT, and (c) HOS-EMD.

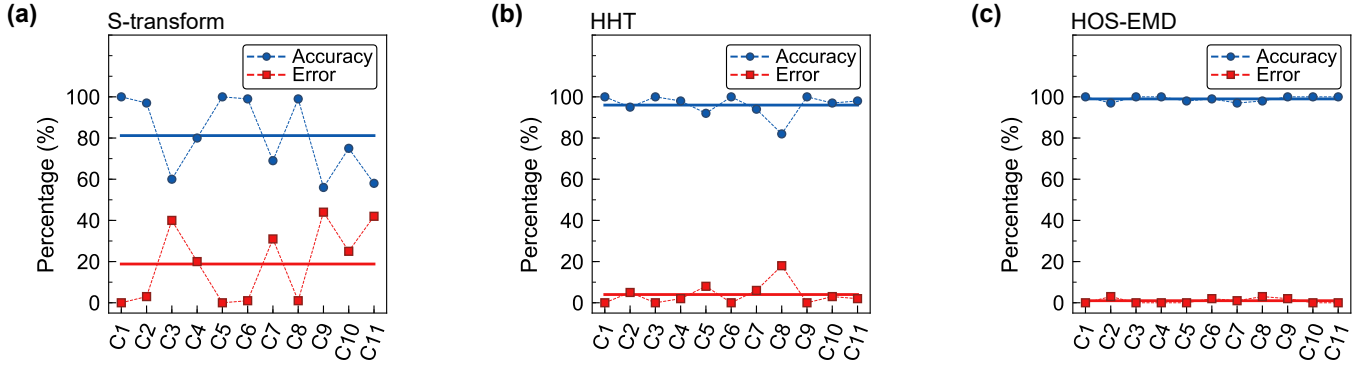


Fig. 10: accuracy and error of different methods: (a) S-transform, (b) HHT, and (c) HOS-EMD.

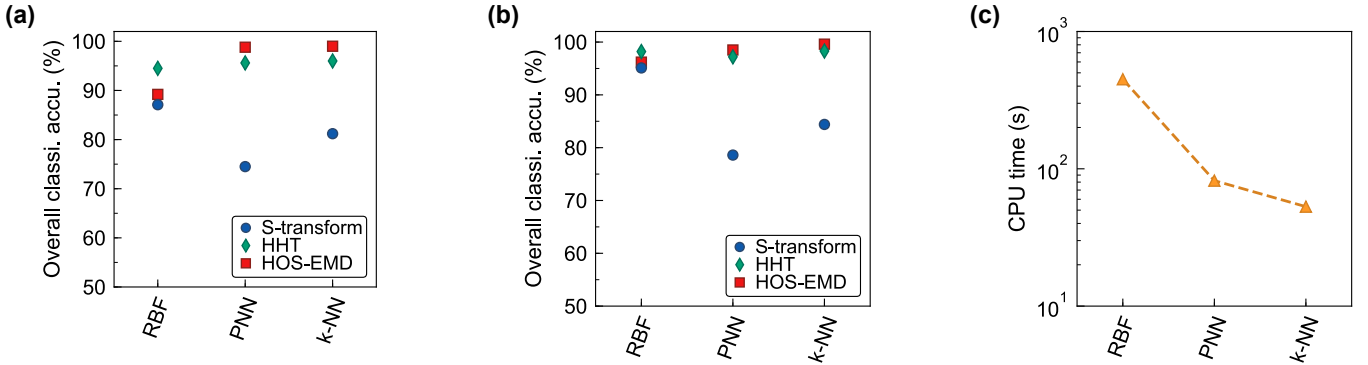


Fig. 11: Classification performance for RBF, PNN and k-NN: (a) accuracy when 35 data in training and 100 data for testing are considered, (b) accuracy when 70 data in training and 200 data for testing are considered, and (c) CPU time requirement for (a).

of the features. In Fig. 12 (a), confusion matrix of the proposed HOS-EMD method with k -NN classifier is shown which is performed with the inclusion of signal to noise ratio (SNR) of 40 dB. It is notable that classification accuracy decreases and error increases due to the inclusion of noise. Overall accuracy is decreased from 99% to 93% according to Fig. 12 (b). Simulation is also performed with the inclusion of 25, 30, 35 and 45 dB of SNR. The overall classification accuracy results for the HOS-EMD along with k -NN classifier are provided in Fig. 13. It shows that the accuracy level decreases with the increase of noise level. But classification results of our proposed method are quite satisfactory till the inclusion of 25dB of SNR.

4 CONCLUSION

The novel contribution of this paper is showing the impact of HOS based features extraction from EMD domain and using k -NN classifier to classify PQ disturbance signals. Only the first three IMFs are considered to derive the outcomes from which HOS termed as variance, skewness and kurtosis are calculated to form an effective feature set. The work here is formulated for eleven class problem. The proposed method is compared to the other methods using S-transform and Hilbert Huang transform along with PNN and RBF classifiers. It is found that the proposed method shows superior performance in classifying different PQ disturbance signals. The robustness of the proposed method is also verified for noisy environment. For further analysis, the proposed method can be employed for online PQ-disturbance classification.

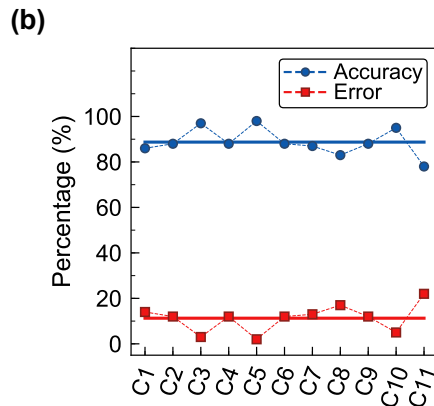
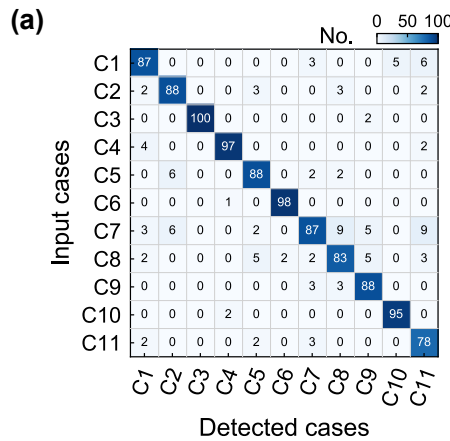


Fig. 12: Performance after inclusion of noise. (a) Confusion matrix, and (b) accuracy and error rate.

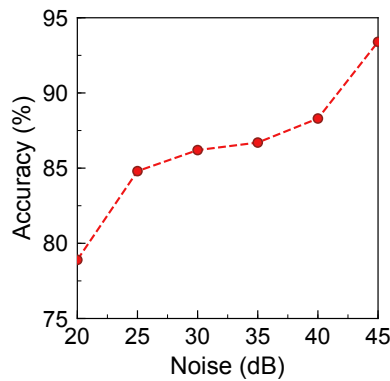


Fig. 13: Impact of SNR on classification accuracy.

5 References

- Mahela, O.P., Shaik, A.G., Gupta, N.: 'A critical review of detection and classification of power quality events', *Renewable and Sustainable Energy Reviews*, 2015, **41**, pp. 495–505
- Mishra, M.: 'Power quality disturbance detection and classification using signal processing and soft computing techniques: A comprehensive review', *Int Trans Electr Energy Syst*, 2018, **0**, (0), pp. e12008
- Hafiz, F., Chowdhury, A.H., Shahnaz, C.: 'An approach for classification of power quality disturbances based on hilbert huang transform and relevance vector machine'. 2012 7th International Conference on Electrical and Computer Engineering. Dhaka, Bangladesh, Dec 2012, pp. 201–204
- Flores, R.A.: 'State of the art in the classification of power quality events, an overview'. 10th International Conference on Harmonics and Quality of Power. Proceedings, Rio de Janeiro, Brazil, Oct 2002, pp. 17–20
- Gaouda, A., Kanoun, S., Salama, M.: 'On-line disturbance classification using nearest neighbor rule', *Electric Power Systems Research*, 2001, **57**, (1), pp. 1–8
- Gu, Y.H., Bollen, M.H.: 'Time-frequency and time-scale domain analysis of voltage disturbances', *IEEE Transactions on Power Delivery*, 2000, **15**, (4), pp. 1279–1284
- Jurado, F., Acero, N., Ogayar, B.: 'Application of signal processing tools for power quality analysis'. IEEE CCECE2002. Canadian Conference on Electrical and Computer Engineering. Conference Proceedings., Manitoba, Canada, May 2002, pp. 82–87
- Poisson, O., Rioual, P., Meunier, M.: 'Detection and measurement of power quality disturbances using wavelet transform', *IEEE transactions on Power Delivery*, 2000, **15**, (3), pp. 1039–1044
- Santoso, S., Grady, W.M., Powers, E.J., Lamoree, J., Bhatt, S.C.: 'Characterization of distribution power quality events with fourier and wavelet transforms', *IEEE Transactions on Power Delivery*, 2000, **15**, (1), pp. 247–254
- Santoso, S., Powers, E.J., Grady, W.M., Parsons, A.C.: 'Power quality disturbance waveform recognition using wavelet-based neural classifier. i. theoretical foundation', *IEEE Transactions on Power Delivery*, 2000, **15**, (1), pp. 222–228
- Zhang, M., Li, K., Hu, Y.: 'Classification of power quality disturbances using wavelet packet energy entropy and ls-svm', *Energy and Power Engineering*, 2010, **2**, (03), pp. 154
- Chandrasekar, P., Kamaraj, V.: 'Detection and classification of power quality disturbance waveform using mra based modified wavelet transform and neural networks', *Journal of Electrical Engineering*, 2010, **61**, (4), pp. 235–240
- Gaouda, A.M., Kanoun, S.H., Salama, M.M.A., Chikhandi, A.Y.: 'Pattern recognition applications for power system disturbance classification', *IEEE Power Engineering Review*, 2002, **22**, (1), pp. 69–70
- Gaig, Z.L.: 'Wavelet-based neural network for power disturbance recognition and classification', *IEEE Transactions on Power Delivery*, 2004, **19**, (4), pp. 1560–1568
- Gargoom, A.M., Ertugrul, N., Soong, W.L.: 'Automatic classification and characterization of power quality events', *IEEE Transactions on Power Delivery*, 2008, **23**, (4), pp. 2417–2425
- Mishra, S., Bhende, C.N., Panigrahi, B.K.: 'Detection and classification of power quality disturbances using s-transform and probabilistic neural network', *IEEE Transactions on Power Delivery*, 2008, **23**, (1), pp. 280–287
- Gargoom, A.M., Ertugrul, N., Soong, W.L.: 'Investigation of effective automatic recognition systems of power-quality events', *IEEE Transactions on Power Delivery*, 2007, **22**, (4), pp. 2319–2326
- Feilat, E.A.: 'Detection of voltage envelope using prony analysis-hilbert transform method', *IEEE Transactions on Power Delivery*, 2006, **21**, (4), pp. 2091–2093
- Kabir, M.A., Shahnaz, C.: 'Denoising of ecg signals based on noise reduction algorithms in emd and wavelet domains', *Biomedical Signal Processing and Control*, 2012, **7**, (5), pp. 481–489
- Shukla, S., Mishra, S., Singh, B.: 'Power quality event classification under noisy conditions using emd-based de-noising techniques', *IEEE Transactions on Industrial Informatics*, 2014, **10**, (2), pp. 1044–1054
- Shukla, S., Mishra, S., Singh, B.: 'Empirical-mode decomposition with hilbert transform for power-quality assessment', *IEEE Transactions on Power Delivery*, 2009, **24**, (4), pp. 2159–2165
- Jayasree, T., Harrison, D.S., Rangaraja, T.S.: 'Automated classification of power quality disturbances using hilbert huang transform and rbf networks', *International Journal of Soft Computing and Engineering*, 2011, **1**, (5), pp. 217–223
- Elango, M., Nirmal Kumar, A., Purushothaman, S.: 'Application of neural networks for power quality disturbance classification using hilbert huang transform', *European Journal of Scientific Research*, 2010, **47**, (3), pp. 442–454
- Chakravorti, T., Patnaik, R.K., Dash, P.K.: 'Advanced signal processing techniques for multiclass disturbance detection and classification in microgrids', *IET Science, Measurement & Technology*, 2017, **11**, (4), pp. 504–515
- Alam, S.S., Bhuiyan, M.I.H.: 'Detection of seizure and epilepsy using higher order statistics in the emd domain', *IEEE Journal of Biomedical and Health Informatics*, 2013, **17**, (2), pp. 312–318
- Acharya, U.R., Sree, S.V., Suri, J.S.: 'Automatic detection of epileptic eeg signals using higher order cumulant features', *International Journal of Neural Systems*, 2011, **21**, (05), pp. 403–414
- Panigrahi, B., Pandi, V.R.: 'Optimal feature selection for classification of power quality disturbances using wavelet packet-based fuzzy k-nearest neighbour algorithm', *IET Generation, Transmission & Distribution*, 2009, **3**, (3), pp. 296–306
- Lin, W.M., Wu, C.H., Lin, C.H., Cheng, F.S.: 'Detection and classification of multiple power-quality disturbances with wavelet multiclass svm', *IEEE Transactions on Power Delivery*, 2008, **23**, (4), pp. 2575–2582
- Achlerkar, P.D., Samantaray, S., Manikandan, M.S.: 'Variational mode decomposition and decision tree based detection and classification of power quality disturbances in grid-connected distributed generation system', *IEEE Transactions on Smart Grid*, 2018, **9**, (4), pp. 3122–3132
- Hafiz, F.: 'Method for Classification of Power Quality Disturbances exploiting Higher Order Statistics in the EMD Domain'. *M.Sc. Thesis*, Bangladesh University of Engineering and Technology, Dhaka, Bangladesh, 2013
- Eristi, H., Yildirim, Ö., Eristi, B., Demir, Y.: 'Automatic recognition system of underlying causes of power quality disturbances based on s-transform and extreme learning machine', *International Journal of Electrical Power & Energy Systems*, 2014, **61**, pp. 553–562
- Manjula, M., Mishra, S., Sarma, A.V.R.S.: 'Empirical mode decomposition with hilbert transform for classification of voltage sag causes using probabilistic neural network', *International Journal of Electrical Power & Energy Systems*, 2013, **44**, (1), pp. 597–603